Interaction of Cholesterol with Various Glycerophospholipids and Sphingomyelin†

Mantripragada B. Sankaram* and Thomas E. Thompson
Department of Biochemistry, University of Virginia Health Sciences Center, Charlottesville, Virginia 22908
Received February 7, 1990; Revised Manuscript Received August 28, 1990

ABSTRACT: The influence of cholesterol on the phase behavior of glycerophospholipids and sphingomyelins was investigated by spin-label electron spin resonance (ESR) spectroscopy. 4-(4,4-Dimethyl-3-oxy-2-tridecyl-2-oxazolidinyl)butanoic acid (5-SASL) and 1-stearoyl-2-[4-(4,4-dimethyl-3-oxy-2-tridecyl-2-oxazolidinyl)butanoyl]-*sn*-glycero-3-phosphocholine (5-PCSL) spin-labels were employed for this purpose. The outer hyperfine splitting constants, A_{max}, measured from the spin-label ESR spectra as a function of temperature were taken as empirical indicators of cholesterol-induced changes in the acyl chain motions in the fluid state. The A_{max} values of 5-PCSL exhibit a triphasic dependence on the concentration of cholesterol for phosphatidylcholines and bovine brain sphingomyelin. We interpret this dependence as reflecting the existence of liquid-disordered, l_d, liquid-ordered, l_o, and coexistence regions, $l_d + l_o$. The phase boundary between the l_d and the two-phase region and the boundary between the l_o and the two-phase region in the phosphatidylcholine–cholesterol systems coalesce at temperatures 25–33 °C above the main-chain melting transition temperature of the cholesterol-free phosphatidylcholine bilayers. In the case of bovine brain sphingomyelin, the $l_d - l_o$ phase coalescence occurs about 47 °C above the melting temperature of the pure sphingomyelin. The selectivity of interaction of cholesterol with glycerophospholipids of varying headgroup charge was studied by comparing the cholesterol-induced changes in the A_{max} values of derivatives of phosphatidylcholine, phosphatidic acid, phosphatidylethanolamine, phosphatidylglycerol, and phosphatidylserine spin-labeled at the fifth position of the *sn*-2 chain. The A_{max} data were analyzed assuming (a) an equimolar stoichiometry for the phospholipid–cholesterol association and (b) that the chemical exchange between cholesterol-associated and cholesterol-free phospholipids in a bilayer is fast on the ESR time scale. The relative strength of cholesterol association with glycerophospholipids of varying chain length and chain composition and with sphingomyelins was assessed by analyzing the A_{max} data of 5-SASL in seven glycerophospholipid and three sphingomyelin multilayers. The results indicate that the interaction of cholesterol with sphingomyelin is the strongest. Increasing headgroup negative charge leads to a stronger association of cholesterol with phospholipids.

Cholesterol is a major lipid component of many biological membranes and its structural role has been the subject of much speculation. Magnetic resonance studies on cholesterol-containing lipid bilayers have suggested that cholesterol fluidizes the gel phase and has a condensing effect on the liquid-crystalline phase of lipid bilayers. Electron spin resonance (ESR)[1] spectroscopic studies (Recktenwald & McConnell, 1981) of headgroup spin-labeled phosphatidylcholine in dimyristoylphosphatidylcholine (DMPC)–cholesterol and dipalmitoylphosphatidylcholine (DPPC)–cholesterol systems have suggested that there are two different liquid crystalline phases that exhibit a coexistence range between 10 and 25 mol % cholesterol. These two phases have been referred to as liquid-disordered (l_d) and liquid-ordered (l_o) phases, respectively, in discussing magnetic resonance spectroscopic results on the differential phospholipid acyl chain motional restriction induced by cholesterol (Ipsen et al., 1987). The two boundary lines separating the l_d phase, the $l_d + l_o$ coexistence region, and the l_o phase are not vertical on the phase diagrams (Recktenwald & McConnell, 1981; Sperotto et al., 1989), indicating that no compound formation occurs in either phase. Based on a theoretical study, it has been proposed recently for the DPPC–cholesterol system that the l_d and l_o phases become miscible at a critical temperature above the main gel to fluid phase transition temperature (Ipsen et al., 1987; Sperotto et al., 1989).

Fluid phase immiscibility such as that proposed for binary phospholipid–cholesterol mixtures could lead to lateral in-plane phase separation in biological membranes. Such phase separation could lead to an efficient demixing of the various protein components of the membrane. However, most experimental and theoretical investigations on the effect of cholesterol have been carried out on dipalmitoylphosphatidylcholine–cholesterol mixtures. In an effort to understand better the effect of cholesterol on phospholipid phase behavior and on phospholipid dynamics, we have carried out a systematic spin-label ESR investigation on binary phospholipid–cholesterol mixtures utilizing a number of dif-

† This research was supported by a grant from the National Institutes of Health (GM-14628).

[1] Abbreviations: DMPC, 1,2-dimyristoyl-*sn*-glycero-3-phosphocholine; DPPC, 1,2-dipalmitoyl-*sn*-glycero-3-phosphocholine; DSPC, 1,2-distearoyl-*sn*-glycero-3-phosphocholine; ESR, electron spin resonance; EDTA, ethylenediaminetetraacetic acid; NMR, nuclear magnetic resonance; Pipes, piperazine-*N*,*N*′-bis(2-ethanesulfonic acid); POPA, 1-palmitoyl-2-oleoyl-*sn*-glycero-3-phosphoric acid; POPC, 1-palmitoyl-2-oleoyl-*sn*-glycero-3-phosphocholine; POPE, 1-palmitoyl-2-oleoyl-*sn*-glycero-3-phosphoethanolamine; POPG, 1-palmitoyl-2-oleoyl-*sn*-glycero-3-phosphoglycerol; POPS, 1-palmitoyl-2-oleoyl-*sn*-glycero-3-phosphoserine; 5-PASL, 1-stearoyl-2-[4-(4,4-dimethyl-3-oxy-2-tridecyl-2-oxazolidinyl)butanoyl]-*sn*-glycero-3-phosphoric acid; 5-PCSL, 1-stearoyl-2-[4-(4,4-dimethyl-3-oxy-2-tridecyl-2-oxazolidinyl)butanoyl]-*sn*-glycero-3-phosphocholine; 5-PESL, 1-stearoyl-2-[4-(4,4-dimethyl-3-oxy-2-tridecyl-2-oxazolidinyl)butanoyl]-*sn*-glycero-3-phosphoethanolamine; 5-PGSL, 1-stearoyl-2-[4-(4,4-dimethyl-3-oxy-2-tridecyl-2-oxazolidinyl)butanoyl]-*sn*-glycero-3-phosphoglycerol; 5-PSSL, 1-stearoyl-2-[4-(4,4-dimethyl-3-oxy-2-tridecyl-2-oxazolidinyl)butanoyl]-*sn*-glycero-3-phosphoserine; 5-SASL, 4-(4,4-dimethyl-3-oxy-2-tridecyl-2-oxazolidinyl)butanoic acid; SPM, sphingomyelin.

0006-2960/90/0429-10670$02.50/0

ferent phospholipids. The questions specifically addressed are, what is the effect of cholesterol on the phase behavior of glycerophospholipids and sphingomyelin? What is the dependence of the strength of association of cholesterol with phospholipids on lipid headgroup structure and acyl chain composition? Is the phase behavior related to the intermolecular pairwise interactions between the constituent molecules?

Experimental Procedures

Materials. Dimyristoylphosphatidylcholine (DMPC), dipalmitoylphosphatidylcholine (DPPC), distearoylphosphatidylcholine (DSPC), 1-palmitoyl-2-oleoylphosphatidic acid (POPA), 1-palmitoyl-2-oleoylphosphatidylcholine (POPC), 1-palmitoyl-2-oleoylphosphatidylethanolamine (POPE), 1-palmitoyl-2-oleoylphosphatidylglycerol (POPG), and 1-palmitoyl-2-oleoylphosphatidylserine (POPS) were from Avanti Polar Lipids (Birmingham, AL). Cholesterol was obtained from Nu-Chek-Prep. (Elysian, MN). Bovine brain, bovine erythrocyte, and chicken egg yolk sphingomyelins were from Sigma Chemical Co. (St. Louis, MO). The stearic acid spin-label, 5-SASL, was purchased from Aldrich Chemical Co. (Milwaukee, WI). The phosphatidylcholine spin-label labeled at the fifth position in the *sn*-2 chain, 5-PCSL, was synthesized by acylation of 1-stearoyl-*sn*-glycero-3-phosphocholine (Avanti Polar Lipids) with 5-SASL in the presence of dicyclohexylcarbodiimide by using 4-pyrrolidinopyridine (Aldrich Chemical Co.) as a catalyst (Mason et al., 1981). The phosphatidic acid (5-PASL), phosphatidylethanolamine (5-PESL), phosphatidylglycerol (5-PGSL), and phosphatidylserine (5-PSSL) spin-labels were synthesized from 5-PCSL by a headgroup exchange reaction catalyzed by phospholipase D (Boehringer-Mannheim, Indianapolis, IN) according to the method of Comfurius and Zwaal (1977).

Sample Preparation. Required quantities of phospholipid, cholesterol, and spin-label (~1 mol %) were dissolved in a 2:1 (v/v) mixture of chloroform and methanol. The solvent was evaporated under a stream of nitrogen gas to form a thin film in a round-bottom flask. The thin film was dried overnight under vacuum to remove any traces of the organic solvents. The lipid multilayers were formed by hydrating the mixtures with 100 μL of buffer (10 mM Pipes, 50 mM KCl, 0.5 mM EDTA, and 0.02% NaN_3, pH 7.0) and vortexing thoroughly at 50 °C. The dispersions were transferred to 100-μL capillaries, which were used as sample cells for ESR spectroscopy.

ESR Spectroscopy. The 100-μL capillaries containing the lipid dispersions were introduced into a quartz tube (Wilmad Glass Co., Buena, NJ). The outer quartz tube contained thin silicon oil to provide better thermal contact. The actual temperature of the sample was measured (±0.1 °C) with a fine-wire thermocouple (Cole-Parmer) inserted in the silicon oil in the outer quartz tube and positioned close to the bottom of the sample. Cavity temperatures were controlled by using a calibrated Varian variable-temperature controller. ESR spectra were recorded on a Varian Associates E-line Century Series 9-GHz spectrometer. Spectra were digitized and stored on an AT&T personal computer by using the interfacing protocol described by Morse (1987). The outer hyperfine splitting constants (A_{max}) were measured directly from the spectra and were half the difference in the magnetic field corresponding to the low-field maxima and the high-field minima. The A_{max} values measured from spectra of independently prepared samples were averaged over two such determinations. The reproducibility in them is estimated to be ±0.1 G. Therefore, the error in the incremental A_{max} values induced by cholesterol, ΔA_{max}, is ±0.2 G.

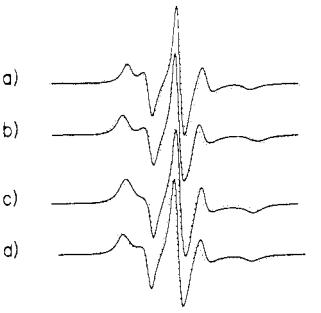

FIGURE 1: ESR spectra at 50 °C of 5-PCSL (a and b), 5-SASL (c and d), spin-labels in DPPC (a and c), and bovine brain sphingomyelin (b and d) bilayers in the presence (dotted line) and absence (solid line) and 30 mol % cholesterol. Buffers: 10 mM Pipes, 50 mM KCl, 0.5 mM EDTA, 0.02% NaN_3, pH 7.0 (5-PCSL) and pH 8.5 (5-SASL). Spectral width: 100 G.

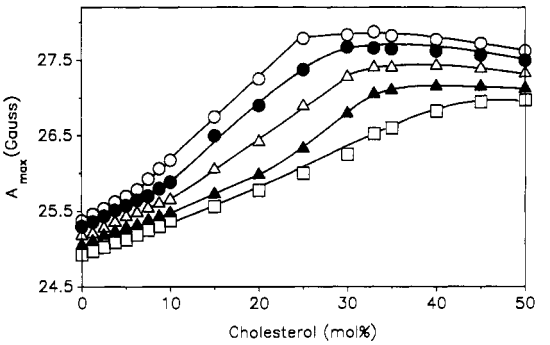

FIGURE 2: Dependence of the outer hyperfine splitting constants, A_{max}, of 5-PCSL-labeled DPPC–cholesterol mixtures on the concentration of cholesterol. The temperatures correspond to 45 °C (○), 50 °C (●), 55 °C (△), 65 °C (▲), and 75 °C (□). Buffer: 10 mM Pipes, 50 mM KCl, 0.5 mM EDTA, 0.02% NaN_3, pH 7.0.

Results

Hyperfine Splitting Constants for Phosphatidylcholine–Cholesterol Bilayers. The ESR spectrum of the phosphatidylcholine spin-label, 5-PCSL, in the fluid phase of DPPC multibilayers in the presence and absence of 30 mol % cholesterol is shown in Figure 1a. The spectra of pure DPPC bilayers in the fluid phase at 50 °C are characteristic of axial symmetry and partial motional averaging. Interaction with cholesterol leads to broader spectra with increased outer hyperfine splitting constants corresponding to an increased motional restriction of the spin-labeled chains.

The outer hyperfine splitting constants, A_{max}, of 5-PCSL incorporated into DPPC–cholesterol mixtures were monitored as a function of cholesterol concentration at various temperatures above the gel to fluid phase transition (Figure 2). The curves at constant temperatures in Figure 2 are complex in shape, especially at lower temperatures. In these cases, a break in the positive slope is evident around 5 mol % cholesterol and the slope becomes negative near 25 mol % cholesterol. These two characteristic cholesterol concentrations are more difficult to discern as the temperature increases; at temperatures above 75 °C, the two points appear to have coalesced. This coalescence is suggested by a virtually linear dependence of A_{max} on the concentration of cholesterol at temperatures above 75 °C. The characteristic concentrations below this temperatures were identified by the following criteria. The low concentration characteristic was taken as the point where the line abruptly changes slope. In order to define the high concentration characteristic point as accurately as possible, the A_{max} versus temperature curves shown in Figure 2 were fit to a fourth-order polynomial function whose derivatives were calculated (Press et al., 1986). The high concentration point was identified as

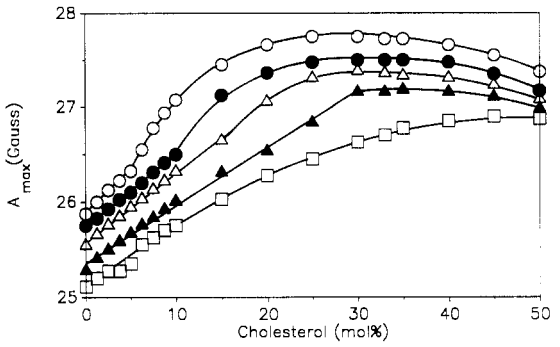

FIGURE 3: Dependence of the outer hyperfine splitting constants, A_{max}, of 5-PCSL-labeled bovine brain sphingomyelin–cholesterol mixtures on the concentration of cholesterol. The temperatures correspond to 45 °C (○), 55 °C (●), 65 °C (△), 75 °C (▲), and 85 °C (□). Buffer: 10 mM Pipes, 50 mM KCl, 0.5 mM EDTA, 0.02% NaN_3, pH 7.0.

the zero crossover point in the derivative. Alternatively, the characteristic point was located with good precision by interpolation using a polynomial or cubic spline algorithm to yield a large enough data set to give a smooth derivative. The loci of the characteristic points for DPPC–cholesterol and for sphingomyelin–cholesterol are shown in Figure 6. The interpretation of these curves is deferred to the Discussion section.

The ESR spectra of the fatty acid spin-label, 5-SASL, in DPPC bilayers in the presence and absence of 30 mol % cholesterol are shown in Figure 1c. The cholesterol-induced spectral changes are very similar to those obtained with the phosphatidylcholine spin-label, 5-PCSL. The ESR spectra of both 5-SASL and 5-PCSL in DMPC and DSPC bilayers above their respective gel to liquid-crystalline phase transition temperatures respond to the addition of cholesterol in a similar way (data not shown). The dependence of the outer hyperfine splitting constants, A_{max}, of 5-PCSL on the concentration of cholesterol incorporated into DMPC and DSPC bilayers was also found to parallel that observed for the DPPC–cholesterol system. The temperatures at which the characteristic concentrations of cholesterol appear to coalesce are 50 °C for DMPC and 85 °C for DSPC.

Hyperfine Splitting Constants for Bovine Brain Sphingomyelin–Cholesterol Bilayers. The ESR spectra of 5-PCSL and 5-SASL spin-labels in the fluid phase of bovine brain sphingomyelin multibilayers in the presence and absence of 30 mol % cholesterol are shown in Figure 1b,d. The spectra of the spin-labels in cholesterol-free sphingomyelin bilayers are qualitatively similar to those in pure DPPC bilayers (Figure 1a,c). However, at a given temperature, the A_{max} values for sphingomyelin are larger than those for the three glycerophosphocholines studied above. Addition of cholesterol induces broader spectra with increased A_{max} values in the sphingomyelin system, similar to those observed in the case of DPPC. The dependence of A_{max} of 5-PCSL on the concentration of cholesterol at various temperatures in the fluid phase is shown in Figure 3. The curves shown in Figure 3 are clearly triphasic up to 65 °C, suggesting the presence of two characteristic cholesterol concentrations of sudden slope change. Between 65 and 85 °C, the low characteristic cholesterol concentration is not readily resolvable but the high characteristic concentration is still discernible. At temperatures higher than 85 °C, A_{max} of 5-PCSL increases nearly linearly with the concentration of cholesterol.

The Behavior of Different Phospholipid Spin-Labels in DPPC Bilayers Containing 30 mol % Cholesterol. The ESR spectra in DPPC multibilayers at 50 °C of spin-labeled derivatives of phosphatidylserine (5-PSSL), phosphatidic acid (5-PASL), and phosphatidylcholine (5-PCSL) spin-labeled at the fifth carbon atom in the *sn*-2 chain are shown in Figure 4. For this set of experiments, we have chosen the temperature and the concentration of cholesterol so that the system is in a single phase region (vide infra). The outer hyperfine splitting constants, A_{max}, and line shapes of all the spectra are very similar, reflecting the random and homogeneous distribution of the spin-labels in DPPC host bilayers. Addition of 30 mol % cholesterol leads to significant changes in the spectra. The A_{max} values increase in all the cases with an accompanying line broadening (dotted lines, Figure 4). The A_{max} data for the phosphatidylserine (5-PSSL), phosphatidylglycerol (5-PGSL), phosphatidic acid (5-PASL), phosphatidylethanolamine (5-PESL), and phosphatidylcholine (5-PCSL) spin-labels in the DPPC host at 50 °C in the absence and presence of 30 mol % cholesterol are shown in Table I. The cholesterol-induced increase in A_{max} and ΔA_{max} is dependent on the type of label employed (Table I). The ΔA_{max} values decrease in the order PS > PG > PA > PE = PC.

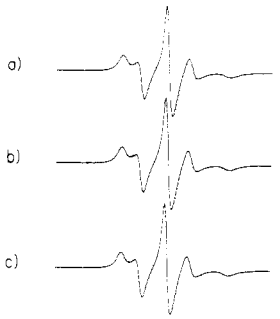

FIGURE 4: ESR spectra at 50 °C of (a) 5-PSSL-, (b) 5-PASL-, and (c) 5-PCSL-labeled DPPC bilayers in the presence (dotted line) and absence (solid line) of 30 mol % cholesterol. Buffer: 10 mM Pipes, 50 mM KCl, 0.5 mM EDTA, 0.02% NaN_3, pH 7.0. Spectral width: 100 G.

Table I: Outer Hyperfine Splitting Constants[a] (A_{max}) and Relative Association Constants (K_r^{PL}) of Glycerophospholipid Spin-Labels Labeled at the Fifth Position of the *sn*-2 Chain, Incorporated into Pure DPPC Bilayers and into DPPC–Cholesterol Mixtures[b]

spin-label	A_{max} (G)	ΔA_{max} (G)	K_r^{PL}
5-PSSL	25.3	2.6	2.5 (0.5)
5-PGSL	25.3	2.4	2.0 (0.4)
5-PASL	25.3	2.2	1.7 (0.3)
5-PESL	25.2	1.8	1.1 (0.2)
5-PCSL	25.3	1.7	1.0

[a] A_{max} and ΔA_{max} values are accurate to ±0.1 and ±0.2 G, respectively. [b] ΔA_{max} is the increase in A_{max} induced by 30 mol % cholesterol. Buffer: 10 mM Pipes, 50 mM KCl, 0.5 mM EDTA, 0.02 % NaN_3, pH 7.0. Temperature, 50 °C. The calculated standard deviations in K_r^{PL} are given in parentheses.

The Behavior of the Fatty Acid Spin-Label, 5-SASL, in Various Phospholipid Bilayers Containing 30 mol % Cholesterol. We have monitored cholesterol-induced changes in the A_{max} of the fatty acid spin-label, 5-SASL, in POPC, POPG, POPA, POPS, and POPE bilayers and also in bovine brain, bovine erythrocyte, and chicken egg yolk sphingomyelins dispersed in a Pipes buffer at pH 8.5. The temperature and the concentration of cholesterol were chosen so that all the binary phospholipid–cholesterol mixtures are in a single phase (vide infra). The pK of the carboxylic group of 5-SASL is 6.6 in DMPC–cholesterol (Esmann & Marsh, 1985) and 6.7 in DMPC alone (Horváth et al., 1988). In negatively charged phosphatidylglycerol host matrices, the pK has been found to be 8.0 (Sankaram et al., 1990). Therefore, the spin-label is fully ionized under these experimental conditions. The ESR

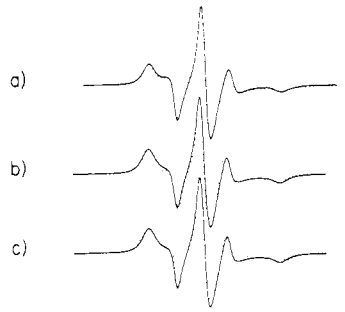

FIGURE 5: ESR spectra at 50 °C of 5-SASL in bilayers formed from (a) bovine brain sphingomyelin, (b) POPG, and (c) POPC in the presence (dotted line) and absence (solid line) of 30 mol % cholesterol. Buffer: 10 mM Pipes, 50 mM KCl, 0.5 mM EDTA, 0.02% NaN_3, pH 8.5. Spectral width: 100 G.

Table II: Outer Hyperfine Splitting Constants[a] (A_{max}) and Relative Association Constants (K_r^{SA}) of 5-SASL Incorporated into Pure Glycerophospholipid and Sphingomyelin Bilayers and into Mixtures of Them with Cholesterol[b]

phospholipid	A_{max} (G)	ΔA_{max} (G)	K_r^{SA}
DMPC	26.3	1.5	3.3 (0.6)
DPPC	26.4	1.5	4.0 (1.1)
POPC	26.6	1.5	6.7 (3.4)
POPE	26.0	1.6	2.7 (0.3)
POPA	26.1	1.3	1.7 (0.6)
POPG	26.2	1.2	1.6 (0.6)
POPS	26.2	1.3	1.9 (0.7)
SPM[c]	26.5	1.4	3.7 (1.8)
SPM[d]	26.5	1.4	3.7 (1.8)
SPM[e]	26.5	1.4	3.7 (1.8)

[a] A_{max} and ΔA_{max} are accurate to ±0.1 and ±0.2 G, respectively. [b] ΔA_{max} is the increase in A_{max} induced by 30 mol % cholesterol. Buffer: 10 mM Pipes, 50 mM KCl, 0.5 mM EDTA, 0.02% NaN_3, pH 8.5. Temperature, 50 °C. The calculated standard deviations in K_r^{SA} are given in parentheses. [c] Bovine brain, rich in stearic and nervonic acids. [d] Bovine erythrocytes, rich in lignoceric acid. [e] Chicken egg yolk, rich in palmitic acid.

spectra of 5-SASL at 50 °C in the presence and absence of 30 mol % cholesterol in bilayers formed from POPG, POPC, and bovine brain sphingomyelin are shown in Figure 5. The A_{max} values for these and seven other phospholipid–cholesterol mixtures are given in Table II. Addition of cholesterol leads to significant changes in the A_{max} values of the label. However, the range of ΔA_{max} in the case of 5-SASL (1.2–1.6 G) is much smaller than that observed for the glycerophospholipid spin-labels (1.7–2.6 G).

Discussion

The A_{max} values of the phosphatidylcholine spin-label, 5-PCSL, versus the concentration of cholesterol in DPPC (Figure 2), show two characteristic cholesterol concentrations where the response of A_{max} is either nonlinear or nonmonotonous with respect to the concentration of cholesterol. Similar characteristic cholesterol concentrations have been observed for the DMPC–cholesterol system (Recktenwald & McConnell, 1987) when the line heights of a headgroup spin-labeled phosphatidylcholine analogue were monitored as a function of cholesterol concentration. In another study, the A_{max} values of the fatty acid spin-label, 5-SASL, in DMPC–, DPPC–, and DSPC–cholesterol systems have clearly shown a discontinuity in the range 25–30 mol % cholesterol (Kusumi et al., 1986). Using 5-PCSL, we find a slope discontinuity in the low-concentration range 7–23 mol % cholesterol in addition to a discontinuity in the range 25–33 mol % cholesterol.

The concentrations at which the characteristic cholesterol concentrations occur are dependent on temperature as seen in Figure 2. With increasing temperature, both the low and the high characteristic concentrations occur at increasingly higher concentrations. However, the low characteristic cholesterol concentration is more steeply dependent on temperature than the high characteristic concentration, as shown in Figure 6. At temperatures greater than 75 °C, the A_{max} increases monotonously with cholesterol concentration. The fluid phase immiscibility persists up to 25, 33, and 33 °C above the main-chain melting transition temperatures of DMPC, DPPC, and DSPC, respectively.

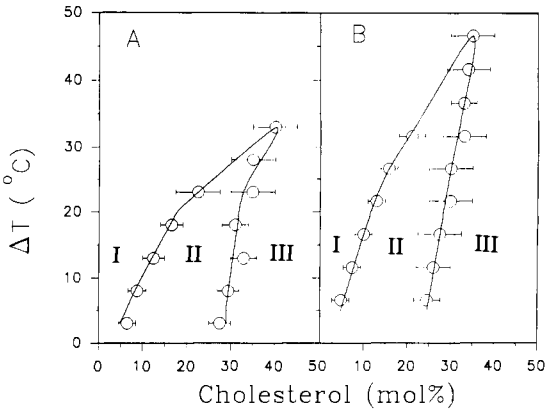

FIGURE 6: Partial phase diagrams of binary mixtures of (A) DPPC and (B) bovine brain sphingomyelin. ΔT is the difference between the temperature of measurement and the corresponding main-chain melting transition of cholesterol-free phospholipid bilayers.

An interesting feature noted in Figure 2 is the maximum in the A_{max} versus temperature curves. This is particularly evident at lower temperatures. A similar observation has been reported in a ^2H NMR study where the quadrupole splittings of choline deuterons in a DPPC–cholesterol mixtures have been monitored as a function of cholesterol concentration (Oldfield et al., 1978). They attribute this effect to a decrease in the packing density of the headgroups caused by a corresponding decrease in the density of the phospholipid molecules in the plane of the membrane. The decrease in A_{max} after the second break point is likely to occur by a similar mechanism. The data in Figure 3 show that the bovine brain sphingomyelin–cholesterol system behaves in a qualitatively similar manner to the DPPC–cholesterol system.

Fluid Phase Immiscibility. If we assume that the characteristic cholesterol concentrations in the curves of Figures 2 and 3 reflect phase changes in the system, then the locus of these points shown in Figure 6 constitutes a phase boundary in a partial phase diagram. We identify the phases following the suggestion of Ipsen et al. (1989) with the l_d in the low cholesterol concentration range (region I), the l_o in the high concentration range (region III), and a coexistence region for both l_d and l_o in the intermediate cholesterol concentration range (region II). Above the maximum in the DPPC-cholesterol curve in Figure 6, l_d and l_o become indistinguishable by our ESR criterion. Hence the maximum is a critical point. The curves for the DMPC– and DSPC–cholesterol systems (data not shown) are quite similar to that obtained for DPPC and may also be interpreted in terms of l_d and l_o phases. As can be seen in Figure 6, the data for sphingomyelin–cholesterol are qualitatively similar to the DPPC–cholesterol data and can be similarly interpreted in terms of l_d and l_o phases. However, the region of coexistence of l_d and l_o is larger and the critical temperature much higher above T_m than it is for DPPC and for the other glycerophospholipids.

Snyder and Freire (1980), using Monte Carlo analysis and heat capacity data, suggested that the nonideality of mixing of cholesterol in the gel phase increases in the order DMPC

= *N*-palmitoylsphingomyelin < DPPC < *N*-lignoceroylsphingomyelin. If it is assumed that the same formalism may be extended to coexisting fluid phases, we see that the order of fluid phase immiscibility (bovine brain sphingomyelin > DSPC = DPPC > DMPC) is in agreement with such a model. The theoretical analysis of the compositional domain structure in phospholipid–cholesterol binary mixtures suggests that the cholesterol-rich domains suddenly become connected at 20 mol % cholesterol. The morphology and connectivity properties of the domains in the liquid-crystalline phase may be expected to be qualitatively similar to those of the gel-phase domains studied by Snyder and Freire (1980).

It is important to note that in the $l_d + l_o$ phase coexistence region the ESR spectra of either 5-SASL or 5-PCSL in any binary mixture of cholesterol with phospholipids investigated here (spectra not shown) are not resolvable into two distinct spectral components corresponding to the l_d and the l_o phases. Two possible explanations can be offered to account for the observation of a single spectrum in the two-phase region. In one, a fast exchange model may be used where the exchange between the two components is assumed to be fast on the ESR time scale (vide infra). This implies that neither phase is long-lived and that the lifetime can be estimated to be shorter than about 30 ms. Alternatively, the ESR spectra from the l_d and the l_o phases can overlap to give the composite spectrum. The ability to discern the component spectra in the experimental spectrum in the phase coexistence region then will be limited by the intrinsic widths of the spectral lines.

Competition between Glycerophospholipid Spin-Labels and DPPC for Cholesterol. The selectivity for cholesterol of the various spin-labeled phospholipids in DPPC bilayers can be analyzed quantitatively, if it is assumed that the ESR spectra of the spin-labels labeled at the fifth position in the acyl chain reflect fast exchange on the ESR time scale. Such an assumption is appropriate since the ESR spectra of the binary mixtures of the phospholipid with cholesterol do not contain two resolvable spectral components. A model can be used in which fast chemical exchange occurs between phospholipids that are not bound to cholesterol and complexes of cholesterol with DPPC with a stoichiometry of n_p moles of cholesterol per mole of DPPC. These complexes have a maximum outer hyperfine splitting constant, A^p, and the remainder of the phospholipids have a lower outer hyperfine splitting constant, A^f, which is taken as that of the pure phospholipid. The outer hyperfine splitting constants were used to characterize the spectra of the spin-labeled phospholipids. Comprehensive line-shape simulations of the ESR spectra from such spin-labels in fluid phase bilayers have shown that there are important contributions from slow molecular motions (Lange et al., 1985; Moser et al., 1989). Thus, the A_{max} values are sensitive to both the amplitude and rate of the phospholipid chain motions and can be used to characterize the strength of interaction of the various spin-labeled phospholipids with cholesterol.

The fast exchange criterion requires that the rate of exchange between the free and cholesterol-associated sites be greater than the difference between the hyperfine splitting constants, A_{max}, of the two spectral components. The A_{max} data in Table I correspond to an upper limit of approximately 4.6 $\times 10^7$ s^{-1}. The exchange rates are formally equivalent to phospholipid translational diffusion rates, which can be calculated from the translational diffusion coefficients by using the Einstein–Smoluchowski relation for a two-dimensional random-walk model. Phospholipid translational diffusion rates thus calculated from lateral diffusion coefficients measured by ESR spectroscopy (Sachse et al., 1987; Rubenstein et al., 1979) and by photobleaching recovery methods (Jovin & Vaz, 1989) for glycerophospholipid bilayers with and without cholesterol in the liquid-crystalline phase are in the range (7–9) $\times 10^7$ s^{-1}. Thus the fast exchange model may be used to analyze the A_{max} data.

With the above model, the following equation, which has been derived for determining the relative association constants in phospholipid–protein recombinants (Sankaram et al., 1989), may be used to determine the association constants of the interaction of cholesterol with various spin-labeled phospholipids relative to 5-PCSL in the DPPC host bilayers, K_r^{PL}:

$$K_r^{PL} = (n_t/n_p - 1)\Delta A_{max}/[(n_t/n_p)\Delta A_{max}(PC) - \Delta A_{max}] \quad (1)$$

where n_t is the total phospholipid:cholesterol mole ratio and $\Delta A_{max}(PC)$ is the differential outer hyperfine splitting constant of 5-PCSL for the DPPC-cholesterol system.

Values of the relative association constants for the different spin-labeled phospholipids, calculated from eq 1, are shown in Table I. To obtain K_r^{PL}, a knowledge of the stoichiometry of the phospholipid–cholesterol complex, n_p, is required. Snyder and Freire (1980) have found that depending on the phospholipid structure, the formation of either a 2:1 phospholipid–cholesterol or an equimolar complex or the coexistence of the two complexes had to be invoked to reproduce theoretically the experimental heat capacity functions. However, we have chosen this to be unity since a direct stoichiometric complex formation with phospholipid can only involve the lone hydroxyl group on cholesterol. It is important to note, however, that the choice of values greater than unity does not affect the comparative analysis of the K_r^{PL} values. It is seen from the data in Table I that the negatively charged phospholipids, PS, PA, and PG, interact more strongly with cholesterol than the zwitterionic phospholipids, PE and PC. The decreasing order of selectivity determined from our ESR spectral analysis, namely, PS > PG > PA > PE = PC, agrees well with those determined by other methods (Demel & de Kruyff, 1976; Blume, 1980; Housley & Stanley, 1982). The greater surface charge in the negatively charged bilayers probably leads to a stronger hydrogen bond between the hydroxyl group in cholesterol and the interfacial region.

Competition between 5-SASL and Different Host Phospholipids for Cholesterol. The A_{max} values of 5-SASL in phospholipid–cholesterol mixtures may be analyzed quantitatively by using the fast exchange model described above. In this case, the equation for the relative association constant, K_r^{SA}, for 5-SASL in a given phospholipid relative to 5-SASL in DPPC is given by (Sankaram et al., 1990)

$$K_r^{SA} = (n_t/n_p - 1)(A^b - A^f)/(A^p - A^b) \quad (2)$$

where A^f, A^b, and A^p are the A_{max} values of 5-SASL in the phospholipid–cholesterol mixtures with stoichiometries of 1:0, n_t:1, and 1:1, respectively.

Values of the relative association constants for 5-SASL in different phospholipid–cholesterol mixtures with a fixed phospholipid:cholesterol mole ratio, have been calculated in this way and are given in Table II. For these calculations, n_p was assumed to be unity as in the case of the glycerophospholipid spin-label data analysis. A^p is not accessible experimentally since stearic acid–cholesterol mixtures do not form bilayers. This value was taken to be $A^f + 1.7$ G. The value of 1.7 G, which is the experimental ΔA_{max} value of 5-PCSL in DPPC–cholesterol, was chosen since it yields a value of unity for K_r^{PL} for 5-PCSL in the DPPC–cholesterol system [see, Sankaram et al. (1990)]. The value of K_r^{SA} obtained for the POPC–cholesterol system is very sensitive to

this choice of parameters, since its value for A_{max} lies very close to that for A^P and therefore small variations in the latter will produce the largest effect on K_r. Thus, the only conclusion that can be drawn for POPC is that the value of K_r^{SA} must be much larger than that for the other phospholipids. However, it should be noted that a different choice for A^P would not affect the relative comparison of the association constants. It should also be emphasized that while a *larger* K_r^{PL} implies a stronger interaction of the labeled phospholipid with cholesterol relative to DPPC, a *smaller* K_r^{SA} implies a stronger interaction of the host phospholipid with cholesterol relative to the host with a larger K_r^{SA}.

The above model assigns all changes in A_{max} to a direct effect of the association of cholesterol with the 5-SASL. Therefore, any other possible effects such as a change in the vertical position of the spin-label in the bulk host lipid or a longer range influence of cholesterol on the bulk order of the phospholipids are included in the specific interaction. The consequences of such effects on the relative association constants have been discussed in detail (Sankaram et al., 1990). To summarize, neglect of factors other than a direct cholesterol–phospholipid association results in the K_r^{SA} values being upper estimates.

The data in Table II for phosphatidylcholines (DMPC, DPPC, and POPC) show that the relative strength of association of cholesterol depends only marginally on chain length. The K_r^{SA} values for 5-SASL in the negatively charged phospholipid bilayers formed from POPS, POPG, and POPA are smaller than those for POPC and POPE, indicating a stronger interaction of cholesterol with the former phospholipids over zwitterionic phospholipids. This result is consistent with the K_r^{PL} data (Table I). However, the selectivities of spin-labeled phospholipids determined in a single host do not necessarily reflect the relative binding strengths of cholesterol to the single isolated phospholipid species. The energetics of association in the former case are primarily determined by the interaction of cholesterol with DPPC.

The three sphingomyelins used in this study have very different chain compositions. The bovine brain sphingomyelin is rich in stearic and nervonic acids, while the bovine erythrocyte and chicken egg yolk sphingomyelins are rich in lignoceroyl and palmitoyl (Estep et al., 1979), respectively. The heterogeneity of the chain composition does not permit any conclusions regarding the effect of chain length and chain unsaturation. It may be noted that similar to the observations made with phosphatidylcholines, the chain composition does not appear to influence the association of cholesterol with sphingomyelin. However, the observation that the ΔA_{max} value for 5-PCSL in sphingomyelin bilayers (1.3 G) is smaller than that in phosphatidylcholine hosts (1.8 G) suggests that cholesterol interacts more strongly with sphingomyelin than with phosphatidylcholines. It is likely that the amide linkage in sphingomyelins, which has a more dipolar character than the corresponding ester linkage in glycerophosphocholines, is responsible for a stronger interaction of cholesterol with sphingomyelin. A possible hydrogen bond between the amide nitrogen and the oxygen atom in the cholesterol hydroxyl group bridged by a water molecule would further strengthen this interaction.

Conclusion

In this paper, we demonstrate that the fluid-phase immiscibility previously observed in the case of DPPC occurs in binary mixtures of cholesterol with other phosphatidylcholines and with bovine brain sphingomyelin. We suggest that the degree of fluid-phase immiscibility is determined primarily by the strength of association of cholesterol with the carbonyl group(s) of the phospholipid hydrocarbon chains. Increasing surface charge is found to increase the strength of association of cholesterol with glycerophospholipids and several sphingomyelins.

Acknowledgments

We would like to thank Dr. Zhao-Qing Wang for the phospholipid spin-label synthesis. We also thank Dr. Rodney Biltonen and Dr. Ching-hsien Huang for helpful suggestions and critical comments on the manuscript.

References

Barenholz, Y., Suurkuusk, J., Mountcastle, D., Thompson, T. E., & Biltonen, R. L. (1976) *Biochemistry 15*, 2441–2447.

Blume, A. (1980) *Biochemistry 19*, 4908–4913.

Comfurius, P., & Zwaal, R. F. A. (1977) *Biochim. Biophys. Acta 488*, 36–42.

Demel, R. A., & de Kruyff, B. (1976) *Biochim. Biophys. Acta 457*, 109–132.

Esmann, M., & Marsh, D. (1985) *Biochemistry 24*, 3572–3578.

Estep, T. N., Mountcastle, D. B., Barenholz, Y., Biltonen, R. L., & Thompson, T. E. (1979) *Biochemistry 18*, 2112–2127.

Horváth, L. I., Brophy, P. J., & Marsh, D. (1988) *Biochemistry 27*, 5296–5304.

Housley, M. D. & Stanley, K. K. (1982) in *Dynamics of Biological Membranes* (Housley, M. D., & Stanley, K. K., Eds.) pp 75–81, Wiley & Sons, New York.

Ipsen, J. H., Karlström, G., Wennerström, K., & Zuckermann, M. J. (1987) *Biochim. Biophys. Acta 905*, 162–172.

Jovin, T., & Vaz, W. L. C. (1989) *Methods Enzymol. 172*, 471–513.

Kusumi, A., Subczynski, W. K., Pasenkiewicz-Gierula, M., Hyde, J. S., & Merkle, H. (1986) *Biochim. Biophys. Acta 854*, 307–317.

Lange, A., Marsh, D., Wassmer, K.-H., Meier, P., & Kothe, G. (1985) *Biochemistry 24*, 4383–4392.

Mason, J. T., Broccoli, A. V., & Huang, C. (1981) *Anal. Biochem. 113*, 96–101.

Morse, P. D. (1987) *Biophys. J. 51*, 440a.

Moser, M., Marsh, D., Meier, P., Wassmer, K.-H., & Kothe, G. (1989) *Biophys. J. 55*, 111–123.

Oldfield, E., Meadows, M., Rice, D., & Jacobs, R. (1978) *Biochemistry 17*, 2727–2740.

Press, W. H., Flannery, B. P., Teukolsky, S. A., & Vetterling, W. T. (1986) *Numerical Recipes*, Cambridge University Press, Cambridge.

Recktenwald, D. J., & McConnell, H. M. (1981) *Biochemistry 20*, 4505–4510.

Rubenstein, J. L. R., Smith, B. A., & McConnell, H. M. (1979) *Proc. Natl. Acad. Sci. U.S.A. 76*, 15–18.

Sachse, J.-H., King, M. D., & Marsh, D. (1987) *J. Magn. Reson. 71*, 385–404.

Sankaram, M. B., de Kruijff, B., & Marsh, D. (1989) *Biochim. Biophys. Acta 986*, 315–320.

Sankaram, M. B., Brophy, P. J., Jordi, W., & Marsh, D. (1990) *Biochim. Biophys. Acta 1021*, 63–69.

Snyder, B., & Freire, E. (1980) *Proc. Natl. Acad. Sci. U.S.A. 77*, 4055–4059.

Sperotto, M. M., Ipsen, J. H., & Mouritsen, O. G. (1989) *Cell Biophys. 14*, 79–95.